Vortragsband der 13. Dreiländertagung D-A-CH 2013
der Windtechnologischen Gesellschaft e.V.
am 10. und 11. Oktober 2013
in Wien

WtG-Berichte Nr. 13

Windeinwirkung in urbaner Umgebung

Christian Bucher (Hrsg.)

Redaktion:
Christian Bucher
Caroline Schneider

2013

Windtechnologische Gesellschaft WtG
Deutschland – Österreich – Schweiz

Somit liegen die Werte aus der Norm auf der sicheren Seite (die ermittelte kritische Geschwindigkeit ist darüber hinaus kleiner). Bevor jedoch die vorliegenden Erkenntnisse auf Bauprojekte übertragen werden können, sind weitere Untersuchungen erforderlich.

7 Literatur (Auszug)

[1] Dielen, B.; Ruscheweyh, H.: Mechanism of Interference galloping of two identical circular Cylinders in Cross Flow, Journal of Wind Engineering and Industrial Aerodynamics, 54/55 (1995), pp. 289-300

[2] DIN EN 1991-1-4 /NA: Einwirkungen auf Tragwerke, Teil 1-4: Allgemeine Einwirkungen - Windlasten, 2010

[3] Igarashi, T. Characteristics of a Flow around two circular Cylinders of different Diameters arranged in Tandem, Bulletin of the JSME; Vol. 25, No. 201, 1982

[4] Jendrzejczyk, J.A.; Chen, S.S.: Fluid Forces on two circular Cylinders in Cross Flow in Flow Induced Vibrations, 1986, ASME, Vol. 194, pp. 1-13

[5] Ruscheweyh, H.: Aeroelastic Interference Effects between slender Structures, Journal of Wind Engineering and Industrial Aerodynamics, 14, 1983, pp. 129-140

[6] Ruscheweyh, H.: Dynamische Windwirkung an Bauwerken, Bd. 2, Bild 4.40, Bauverlag Wiesbaden, 1982

[7] Ruscheweyh, H., Trätner, A.: Winddynamische Interferenzwirkung zwischen großen Schornsteinen, WtG-Berichte Nr. 6, 1999

[8] Zdravkovich, M.M.: Flow Induced Oscillations of two interfering circular Cylinders, Internat. Conf. on Flow Induced Vibrations in Fluid Engineering, Sept. 1982, BHRA Fluid Eng., UK

Aeroelastic stability of a U-shaped profile

J. Strecha[a], J. Dragan[a], L. Spitzy[a], S. Pospíšil[b], R. Král[b], S. Kuznetsov[b,c], H. Steinrück[a]

[a]Institute for Fluid Mechanics and Heat Transfer, Vienna University of Technology
[b]Institute of Theoretical and Applied Mechanics, Academy of Sciences of the Czech Republic
[c]Centre of Excellence Telč, Czech Republic

Abstract: We present the results of an experimental study. The aero-elastic stability of a U-beam with a certain aspect ratio was investigated. Firstly, we examine the possibility of transverse galloping. Therefore, the measured aerodynamic forces acting on a static model are presented. Secondly, we consider two-degree of freedom flutter vibrations and vortex-induced vibrations. Here, another model was mounted on a special test stand that allowed transverse and rotational movement of the model.

We present experimental results regarding the aero-elastic stability of a U-shaped profile with an aspect-ratio (along-wind length B, frontal height H) of $B/H = 4.65$. In the literature [3] it can be found that a square prism ($B/H = 1$) can perform galloping oscillations. However, this is not the case for a flat rectangular prism ($B/H = 10$), [3]. The aspect ratio of the U-beam under consideration here lies between these two values. Additionally, the asymmetry of the profile possibly introduces interesting effects. In a comprehensive study of a $B/H = 4$ rectangular prism [2], it is shown experimentally that vortex-induced as well as self-excited one-degree of freedom vibrations are possible. Our investigation aims at understanding the excitation mechanisms and estimate critical velocities. Simulations and, more recently, wind-tunnel experiments are used in our investigations.

The experiments were conducted at the *Centre of Excellence Telč* (Czech republic). A special test-stand, described in [1] (see figure 1), was used. The closed-loop wind tunnel offered a test-section with a width of 1.9 m and a height of 1.8 m. However, the relevant cross-section was reduced by the test-stand to an area of about $0.65\,\mathrm{m} \times 1.4\,\mathrm{m}$. The aerodynamic forces acting on a static model were measured at the laboratory of the Institute of Fluid Mechanics at the Vienna University of Technology. Here, an open-loop wind tunnel was available. The dimensions of the test-section were $1.2\,\mathrm{m} \times 1.0\,\mathrm{m}$ (width $\times$ height) The simulations were also carried out in Vienna using *CFD*-software package *Ansys-CFX*.

The outline of this contribution is as follows: In an introductory part, we try to estimate the ranges of reduced (dimensionless) velocities where vibrations can be expected. Then, the stability of the profile against transverse galloping oscillations under the quasi-stationary assumption is assessed. We find, that the profile is stable in this particular case. In contrast to this, we present experimental results showing that self-excited two-degree of freedom vibrations can occur. Then, we consider the possibility of vortex-induced vibrations.

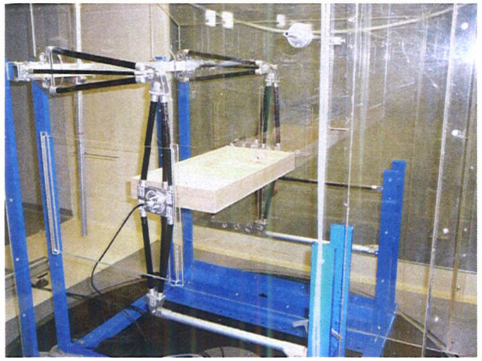

Figure 1: Picture of the test stand with mounted section model (Photo taken at the *Centre of Excellence Telč* by L. Spitzy).

1 Definitions

We consider a U-beam in cross-flow. The aspect ratio (along-wind length B over frontal height H) shall equal $B/H = 4.65$. For the first series of measurements, carried out in Vienna, the model could be inclined. This is shown in figure 2. The second series, carried out in Telč, required that the model can move in vertical direction (y), and rotate (φ). See figure 3.

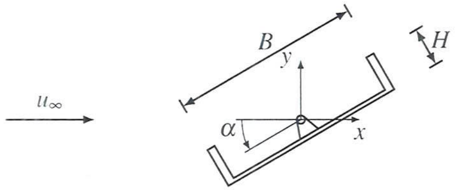

Figure 2: The section model can be inclined. The velocity of the oncoming flow is u_∞.

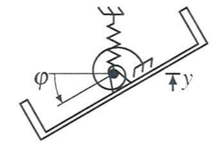

Figure 3: The U-beam has a transverse (heave) and a rotational (pitch) degree of freedom. Its position is described by the vertical displacement y and its angle φ. Spring forces act accordingly.

The breadth of the structure is be much larger than its height or length. Thus, two-dimensional conditions are assumed. The experiments were carried out in turbulent wind tunnels, yet at rather low turbulence intensities. The CFD simulations were carried out using a two-dimensional computational domain and a RANS-Model (the $k\omega$-SST model) was used.

The aerodynamic forces acting on the model were measured with a wind-tunnel scale. The model was fixed to the scale on one end. On the other end, a plate was attached to the model to ensure two-dimensional flow conditions.

For the observation of vibrations the model was allowed to move transverse to the flow and to rotate (see figure 3). Here, the model was mounted on a special test-stand, [1]. The corresponding eigenfrequencies are named $f_{0.y}$ and $f_{0.\varphi}$. Both eigenfrequencies could be adjusted independently.

We form the dimensionless reduced velocity $U^* = \frac{u_\infty}{H f_0}$ with the far-field flow velocity u_∞, the frontal height H and the mechanical eigenfrequency f_0. When not pointed out explicitly, the heave eigenfrequency $f_{0.y}$ is used. If the reduced velocity is written with a subscript (as in U^*_φ), the subscript refers to the respective eigenfrequency. Furthermore, we denote the frequency ratio by $\Omega = f_{0.y}/f_{0.\varphi}$, the Reynolds number by $\mathrm{Re} = \frac{u_\infty H}{\nu}$ and the Strouhal number by $\mathrm{St} = \frac{f_{vs} H}{u_\infty}$.

The vortex shedding frequency f_{vs} was measured for several flow-velocities. The corresponding Strouhal number St as a function of the Reynolds number Re is shown in figure 4. Most experiments were carried out in the range $\mathrm{Re} < 2 \cdot 10^5$. Here, the Strouhal number is approximately $\mathrm{St} \approx 0.14$. Vortex-induced vibrations can be expected when the mechanical eigenfrequency coincides with the vortex shedding frequency, $f_0 \approx f_{vs}$. Given the definitions of the reduced velocity U^* and St, this is the case when $U^* \approx 1/\mathrm{St}$ holds. Thus, vortex-induced vibrations can be expected at $U^* \approx 7.1$. Self-excited flutter can be expected at sufficiently higher reduced velocities.

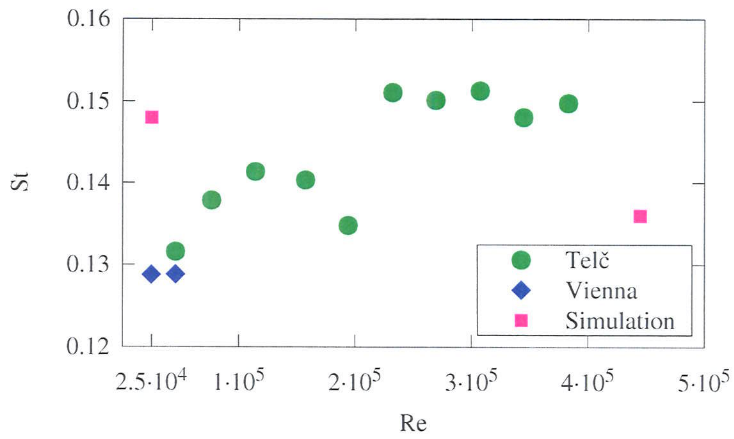

Figure 4: Strouhal number St over Reynolds number Re: Comparison of experiments at the *Centre of Excellence Telč*, the Vienna University of Technology and 2D RANS-Simulations using Ansys CFX.

2 Transverse galloping

The nature of transverse galloping allows, that stability of the structure can be determined easily: The aerodynamic forces on a stationary model, measured at several angles of inclination, suffice to decide whether galloping will occur or not [3], if the influence of vortex shedding can be neglected. This is the case when $f_{vs} \gg f_{0.y}$.

The coefficients of drag, lift and torsional moment for several angles of inclination are shown in figure 5. Here, the forces per unit length were made dimensionless with $\frac{1}{2} H \rho u_\infty^2$, the torsional moment per unit length using $\frac{1}{2} H B \rho u_\infty^2$. The torsional moment is given about the center of the profile's convex hull. For comparison, the measurements were also carried out with a rectangular-prism section model with the same aspect ratio as the U-beam. Both models follow the same trend, yet the force coefficients pertaining to the U-beam have more features, owing to the asymmetry of the model.

The negative slope of the c_L-curve in this representation indicates, that transverse galloping should not occur under the previously made assumptions, [3].

While the simulations agree with the general trend, simulation and experiments disagree quantitatively and in several details. The reasons are most likely the two-dimensional domain in the simulations and some imperfections, such as model deformation in the experiments.

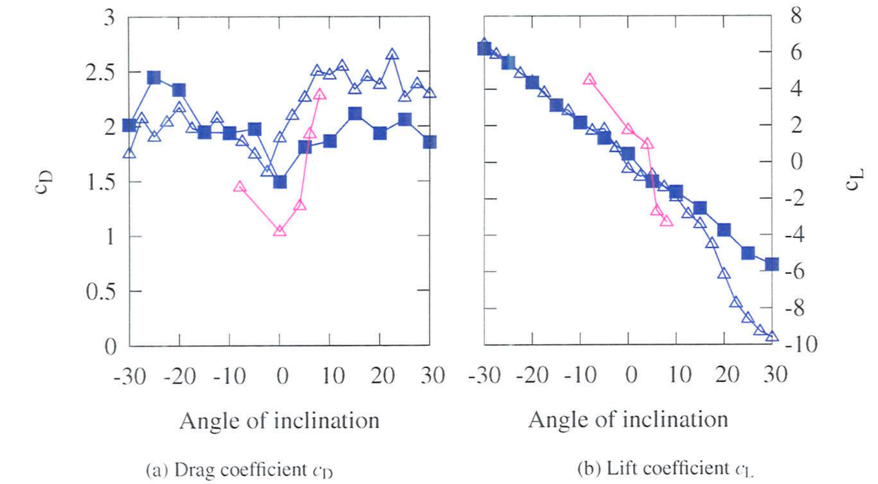

(a) Drag coefficient c_D

(b) Lift coefficient c_L

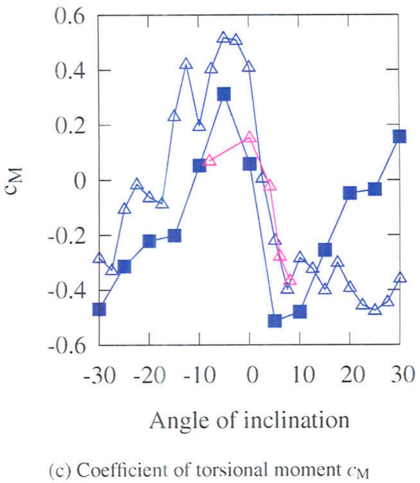

(c) Coefficient of torsional moment c_M

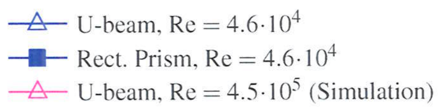

Figure 5: Coefficients of drag (a), lift (b) and torsional moment (c) as measured in Vienna for various angles of attack for a U-beam and a rectangular prism. Lift forces act in y-direction, drag forces in x-direction (see figure 2).

3 Self-excited flutter vibrations

Flutter vibrations were observed at higher reduced velocities and for $\Omega = f_{0.y}/f_{0.\varphi} = 1$. To observe hysteresis loops, the following procedure was chosen: The experiment was started with an initial, low flow velocity. Then, the flow-velocity was increased step-wise. Each flow velocity was maintained for some time. When pronounced vibrations occurred, the flow velocity was

decreased step-wise again, until the initial flow velocity was reached. A time-series of the whole process is shown in figure 6.

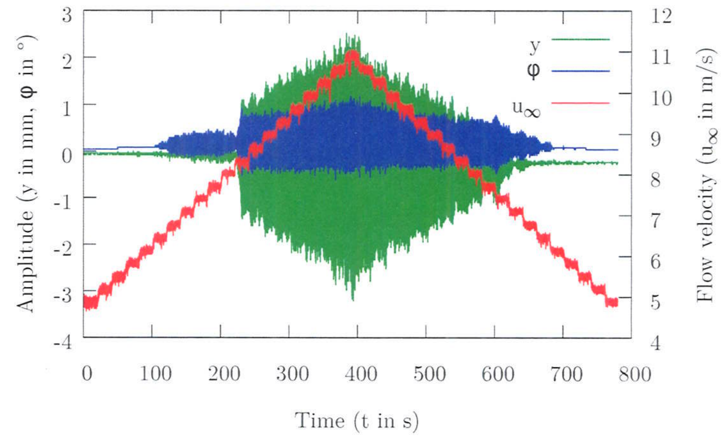

Figure 6: Time-series of a hysteresis-loop experiment ($\Omega = 1$, $f_0 = 6.5$ Hz, see figure 7, b).

The results of two such series with different eigenfrequencies are shown in figure 7. In both cases hysteresis loops can be observed, indicating sub-critical branching. The dimensional critical flow velocities are of similar magnitude for both cases ($u_{\infty.c} = 8.7$ m/s when $f_0 = 4.27$ Hz, and $u_{\infty.c} = 8.3$ m/s when $f_0 = 6.5$ Hz, for increasing flow velocities). However, in the framework of aerodynamic derivatives (which can act as negative damping), there should be a unique critical *reduced* velocity $U_c^* = u_{\infty.c}/(Hf_0)$, given that the damping ratio is constant. Whether a linear approach is not valid in our case, or the damping ratio is not constant cannot be decided conclusively with the available data.

4 Vortex-induced vibrations

The experiments aimed at observing vortex-induced vibrations could only be carried out at rather low flow-velocities. This is a result of the limited range of eigenfrequencies attainable with the used test-stand.

Interestingly, the frequency ratio $\Omega = f_{0.y}/f_{0.\varphi}$ played a significant role. As can be seen in figure 9, an increasing frequency-ratio lead to increasing vibrations. Although the beam had a rotational degree of freedom, no torsional vibrations were excited by the vortex shedding.

In simulations at $U^* = 7.4$, $\Omega = 1$ only minuscule vibrations could be observed, despite the fact that the simulation was carried out without mechanical damping.

Hysteresis loops could also be observed in case of vortex-induced vibrations ($\Omega = 2.2$). See figure 10. For higher flow velocities, self-excited torsional vibrations set in.

The simulations were important for the design of the experiments. However, the long time behaviour of the results depends on the discretization method. This is especially the case when simulating vortex-induced vibrations. The accuracy requirements lead to very long computational times. It is virtually impossible to cover the whole parameter space U^*, Re, Ω, even

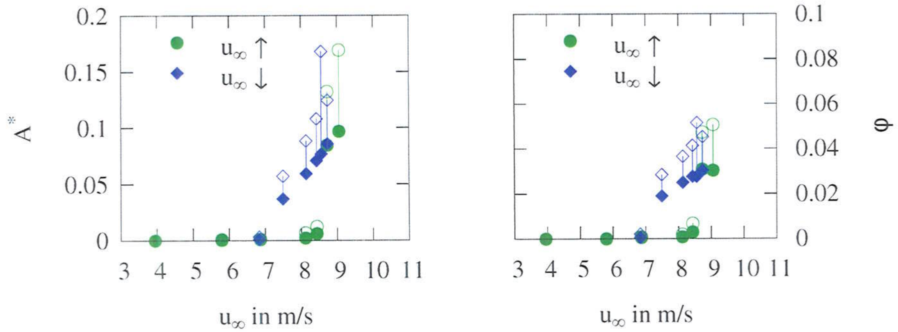

(a) $f_0 = 4.27\,\text{Hz}$, $\Omega = 1$, $7.6 \cdot 10^4 \leq \text{Re} \leq 1.8 \cdot 10^5$, $14.2 \leq U^* \leq 32.6$

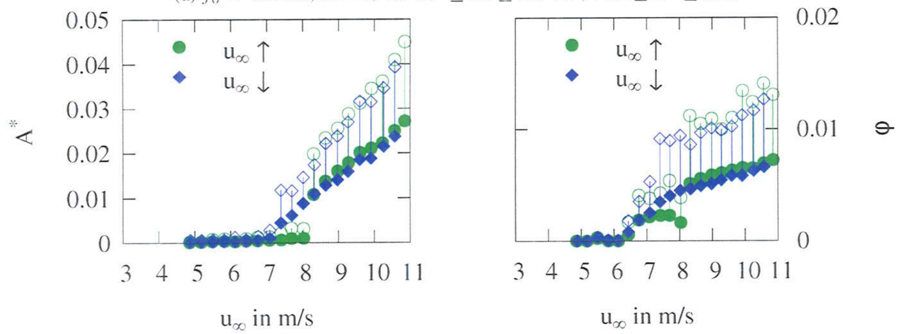

(b) $f_0 = 6.5\,\text{Hz}$, $\Omega = 1$, $9.5 \cdot 10^4 \leq \text{Re} \leq 2.1 \cdot 10^5$, $11.5 \leq U^* \leq 25.7$

Figure 7: Hysteresis loops at higher reduced velocities: Different paths can be observed for increasing and decreasing reduced velocity. The RMS-value of the mean-free displacement and angle is shown. The reduced Amplitude $A^* = y/H$, φ is given in degrees.

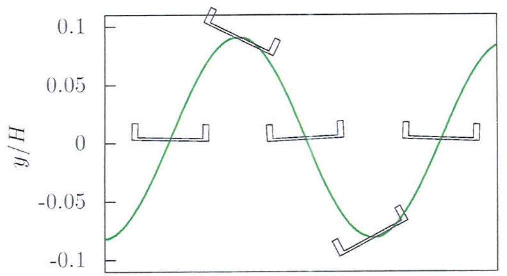

Figure 8: Visualization of the phase between heave and pitch. Experiment at $U^* = 26.7$, $\text{Re} = 7.8 \cdot 10^4$, $\Omega = 1$. The angles were scaled by a factor of two.

without considering mechanical damping. Currently, we are working on a more time efficient discretization scheme.

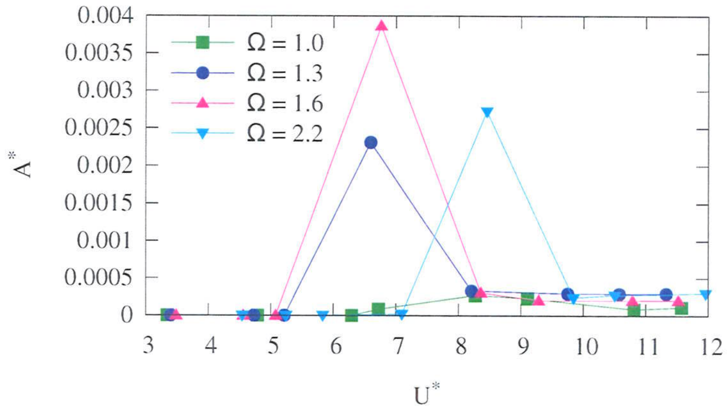

Figure 9: Vortex-induced Vibrations: For increasing frequency ratios ($\Omega = f_{0.y}/f_{0.\varphi}$) vortex-induced vibrations set in. The RMS-value of the mean-free displacement and angle (full symbols) and the respective maximum value (open symbol) are shown. $A^* = y/H$.

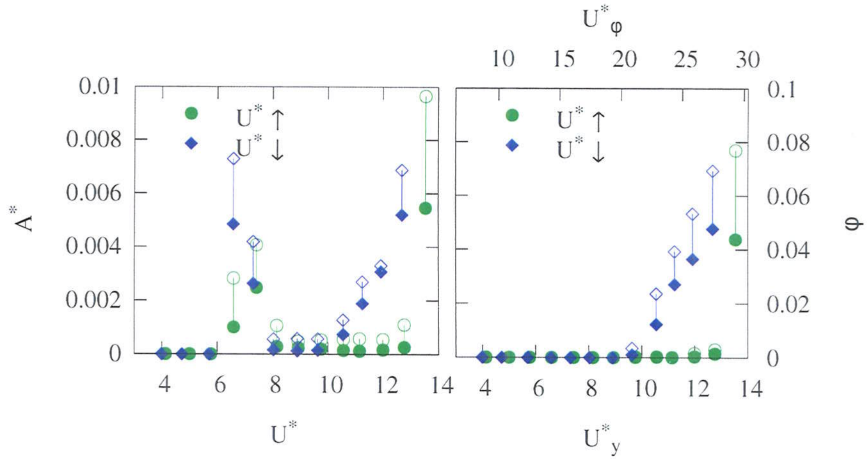

Figure 10: Vortex-induced vibrations: For increasing and decreasing reduced velocities different paths can be observed. The RMS-value of the mean-free displacement and angle (full symbols) and the respective maximum value (open symbol) are shown. In the right diagram (rotation) the reduced velocity is calculated with $f_{0.y}$ (lower x-axis) and $f_{0.\varphi}$ (upper x-axis).

5 Conclusions

We found that the U-beam under consideration will not perform transverse galloping oscillations. However, given the freedom to rotate, more complex flutter oscillations occur. Self excited oscillations were observed at reduced velocities $U^* > 15$ in one case. Pronounced hysteresis phenomena where observed in another case.

It was also seen that vortex shedding can cause vibrations. However, the ratio between heave and pitch eigenfrequencies is important here. It was found that detuning the eigenfrequencies leads to more pronounced vibrations.

Acknowledgements

The experiments were carried out by two students, Lorenzo Spitzy and Johanna Dragan, in the course of their bachelor theses at our institute. The *Centre of Excellence* Telč is co-financed under the Operational Programme Research and Development for Innovation. Funding comes from the European Regional Development Fund and from the Czech state budget. The research was supported by the project CZ.1.05/1.1.00/02.0060 which is co-funded by the European Regional Development Fund.

References

[1] R. Král, S. Pospíšil, and J. Náprstek. "Experimental Set-up for Advanced Aeroelastic Tests on Sectional Models." In: *Experimental Techniques* (2013). In print.

[2] M. Matsumoto et al. "Vortex-induced vibration and its effect on torsional flutter instability in the case of B/D = 4 rectangular cylinder." In: *Journal of Wind Engineering and Industrial Aerodynamics* 96 (2008), pp. 971–983.

[3] M. P. Païdoussis, S. J. Price, and E. de Langre. *Fluid Structure Interactions*. Cambridge University Press, 2011.

Einfluss der Turbulenzparameter auf die Berechnung von Winddrücken mit RANS-CFD-Berechnungen

Prof. Dr.-Ing. Casimir Katz

SOFiSTiK AG, Oberschleißheim

Kurzfassung: Für Anwendungen im Windingenieurwesen mit den hohen Reynoldszahlen müssen Turbulenzen modelliert werden. Nun ist der natürliche Wind anisotrop, d.h. die Turbulenzintensität ist in den drei Koordinatenrichtungen unterschiedlich. Hingegen verwenden die meisten Strömungsberechnungen ein isotropes Turbulenzmodell. Die in der Literatur angegebenen Parameter passen daher nicht so einfach zusammen.
Bei den meistverwendeten k-ε und k-ω Modellen kann man die turbulente kinetische Energie recht gut abschätzen, aber bei der Dissipation entstehen erhebliche Abweichungen. Es werden die in der Literatur befindlichen Angaben gegenüber gestellt und die Auswirkungen an zwei Beispielen numerisch evaluiert.
Bei dem Silsoe-Cube wird eine Strömung im untersten Bereich der atmosphärischen Grenzschicht untersucht. Dort sind sowohl die gemessenen als auch die theoretisch hergeleiteten Integralen Längenmaße deutlich unter den Angaben der Literatur.
Bei dem Querschnitt der Millaubrücke in 200 m Höhe sind hingegen die integralen Längenmaße zwar ähnlich, sie zerfallen aber bei einer numerischen Berechnung bei der Annäherung an das Hindernis, sind also nicht stabil.
Eine abschließende Antwort lässt sich sicher noch nicht geben, jedoch sind die von Richards angegebenen Randbedingungen als im Wesentlichen zutreffend anzusehen.

1 Einführung

„Liebe und andere Turbulenzen" heißt ein Film der derzeit im Kino läuft. So richtig verstanden sind Turbulenzen also immer noch nicht. Zwar kann man heute im Bereich niedriger Reynoldszahlen mit der DNS-Methode Strömungen zutreffend berechnen, aber für den Windingenieur mit den hohen Reynoldszahlen müssen Turbulenzen irgendwie modelliert werden. Nun ist der natürliche Wind anisotrop, d.h. die Turbulenzintensität ist in den drei Koordinatenrichtungen unterschiedlich. Hingegen verwenden nahezu alle Strömungsberechnungen ein isotropes Turbulenzmodell. Einige der sich daraus ergebenden Fragestellungen sollen hier beleuchtet werden.